Angular Resolution Improvement for an 8 meter class Telescope via on-line Sub-aperture Selection

Morossi C., Franchini M., Furlani S.
Osservatorio Astronomico di Trieste
Via G.B. Tiepolo, 11
I-34131 Trieste (Italy)

1 Introduction

The implementation of an Adaptive Optics (AO) system for visual observations with a large diameter telescope is very challenging due to the large number of sub-pupils required to properly sample the incoming wavefront. Furthermore, due to the limited size of coherent cells in the visible, there are severe limitations in the brightness of the target used to feed the wavefront sensor. On the other hand, the situation is much more relaxed in the infrared where r_0 is much larger. Therefore, it is worthwhile to investigate the possibility of improving the performances of an IR AO system in the visible by means of complementary techniques like, for example, on-line image selection.

The problem of improving the image quality of a ground-based telescope by means of co-addition of selected short exposures has been already discussed in several literature papers (e.g. Fried 1966, Hecquet & Coupinot 1985). The main conclusion was that "*At optical wavelengths the technique should be effective when the seeing is good, but not exceptional and with telescopes of one meter diameter*". In fact, the achievable gain in spatial resolution depends on the D/r_0 ratio reaching a maximum in the range $4 < D/r_0 < 7$. Since typical values of the Fried parameter in the visible are $r_0 \approx 10$ cm, it means that no significant improvement can be achieved via image selection technique for the new generation of large diameter telescopes.

In this paper we propose to adopt an on-line multi-aperture selection approach to overcome the problem of the large value of the D/r0 ratio in an 8-meter telescope. We think that this technique can be used to complement an IR AO system. Section 2 describes the implementation of a multi-sub-aperture fast shutter add-on in the optical scheme of an adaptive optics system of a VLT-like telescope. Section 3 presents the numerical simulation we performed to evaluate the achievable gains in Strehl ratio and in spatial resolution assuming different seeing conditions and different magnitudes of the star driving the selection. Section 4 contains the results and conclusions.

2 The sub-aperture system

The typical AO system consists of three main components, namely an adaptive mirror, a wavefront sensor and a control system. We propose to insert in the optical path, after the AO loop a multi-aperture fast shutter driven by a modified AO control unit (see Fig. 1). The fast shutter apertures match in position and size the sub-pupils seen by the wavefront sensor. In the visual range the number of coherent cells in each sub-pupil, which is optimised to work in the infrared, is such that the average tip-tilt slopes of the wavefront measured by the wavefront sensor do not permit a satisfactory wavefront reconstruction. As a consequence, even in closed loop regime, the corrected wavefront in each sub-pupil can differ significantly from the un-aberrated one. It is therefore possible to assign to each sub-pupil image, formed on the wavefront sensor, a One Number Merit Function (ONMF) which depends on the local wavefront flatness. This ONMF, measured from the wavefront data, can then be used to perform an on-line sub-pupil selection by opening or closing the corresponding fast shutter sub-aperture.

Figure 2 shows the superimposition of the fast shutter multi-aperture mask on the telescope pupil of a VLT like telescope. The pupil was divided in 60 circular sub-apertures 90 centimetres in diameter. The size of the sub-pupils was

chosen in such a way to be consistent with a typical IR r_0 and to have a D/r_0 ratio in the visible falling in the useful range for applying image selection. The circular shape and the geometry of the sub-aperture were chosen for simplicity, but different solutions can be achieved to maximise the throughput[1].

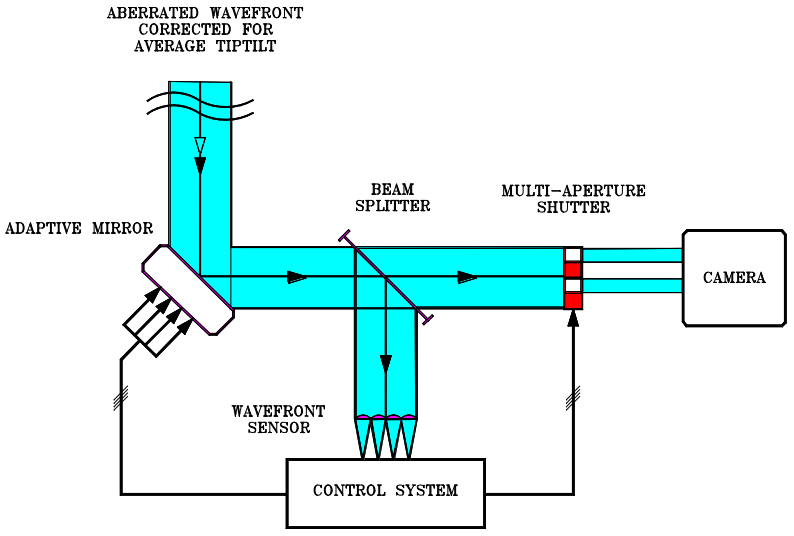

Figure 1: Optical scheme

3 Numerical simulation

To evaluate the performances of an on-line sub-aperture system like that described in the previous section, we wrote a code based on IDL modules. We can divide our simulation into three parts:

- The computation of an input wavefront to mimic the effect of the atmosphere on a long exposure image;
- The evaluation of an ONMF for each sub-aperture;
- The computation of a long exposure image by co-adding individual short exposures taken through a pupil built only with those sub-apertures whose ONMF is better than a given threshold.

3.1 Wavefront simulator

To mimic a long exposure we used the Taylor hypothesis and we computed a rectangular wavefront to be flown above the telescope pupil. The length of the wavefront divided by the wind velocity gives the maximum continuum exposure

[1] See for example Tyler & Stribling (1998) for a different approach to the problem of variable geometry pupil.

time. Several rectangular wavefronts were computed by using the method proposed by Welsh (1997) and each of them has the following characteristics:

- von Karman statistics
- L_0 = 30 m
- r_0 = 0.1, 0.2, 0.3 m
- V_{wind} = 10 m s^{-1}
- Screen size ~ 8x40 m^2
- Screen resol. ~ 0.03 m
- Max exp. time ~ 4 s
- # of screens = 4

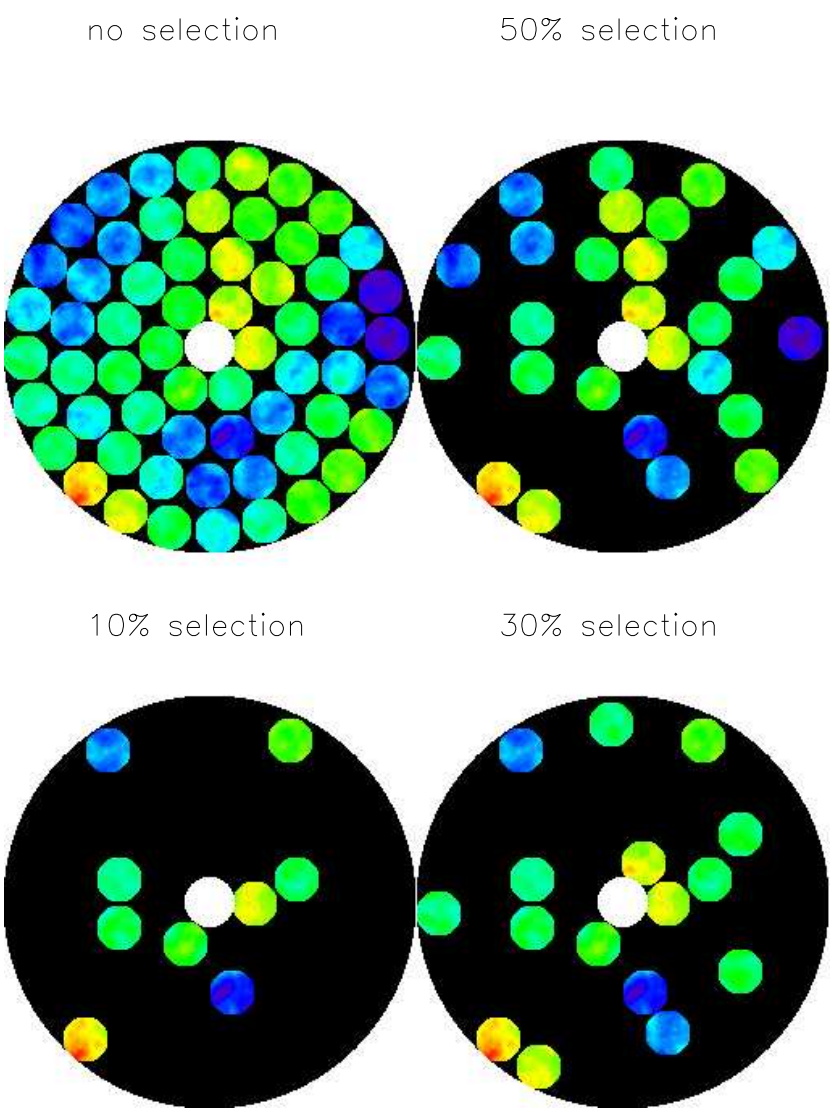

Figure 2: Telescope pupil and sub-aperture mask: 100% (upper-left), 50% (upper-right), 30% (lower-right) and 10% (lower-left) sub-apertures opened.

3.2 The optical system

In simulating the system sketched in Fig.1 we assumed an 8m telescope with a central obstruction of 1m and we sub-divided its pupil in 60 sub-apertures with equivalent diameter of 0.9m.

The wavefront sensor was assumed to be a Shack-Hartmann, which images each sub-pupil on an 8x8-pixel matrix. The control unit measures for each image the centroid position to feed the AO system and the ONMF value to be used for the opening/closing of the shutter sub-apertures.

3.3 Aperture selection

The telescope pupil was moved along the simulated wavefront to generate 1025 snapshots with a step of about 0.03m (i.e. with a time interval of about 4 ms). For each step, we computed the wavefront sensor image of each sub-pupil. While the local tip-tilt is assumed to be completely removed by the AO system, higher order aberrations characterise in different amounts different sub-pupils. An evaluation of the image quality can be obtained by computing one of the several ONMFs proposed by (Muller & Buffington 1974). In our simulation we used:

$$\text{ONMF} = \sum \left(\frac{I}{\sum I} \right)^2$$

Where I is the intensity measured in each pixel of the 8x8 matrix: the higher the ONMF value the better the image quality.

The I values where computed by assuming different V magnitudes of the star seen by the wavefront sensor and taking into account Poisson noise. For each individual wavefront we computed 60x1025 sub-pupil images and ONMFs. By studying the statistical distribution of the ONMF values we determined the ONMF thresholds which select the best 10%, 30% or 50% of the sub-pupils. The control unit compares the actual value of the ONMF for each sub-pupil with the adopted threshold and sends to the shutter a signal to close or open the corresponding sub-aperture for the next snapshot. As a consequence the instantaneous telescope pupil during the long exposure varies. Figure 2 shows the pupils resulting from different threshold selection for one of the 1025 snapshots. It must be noticed that due to statistical reasons, the telescope effective pupil of a long exposure is the same as in the case of no-selection, only the throughput is reduced by the percentage of rejected sub-apertures.

3.4 Long exposure image

The snapshot images obtained by convolving the input wavefront (after removal of local tip-tilts) with the instantaneous pupils (see fig. 2) are co-added to obtain a long exposure image. To increase the photometric stability 4 different sets of 1025 co-added snapshots are averaged.

4 Results and conclusions

Four long exposure images, corresponding to different acceptance thresholds (100%, 50%, 30%, 10%), are constructed for each value of r_0 (0.1, 0.2, 0.3-m) assuming 3 different V magnitudes (10, 12, 14) of the point source used to

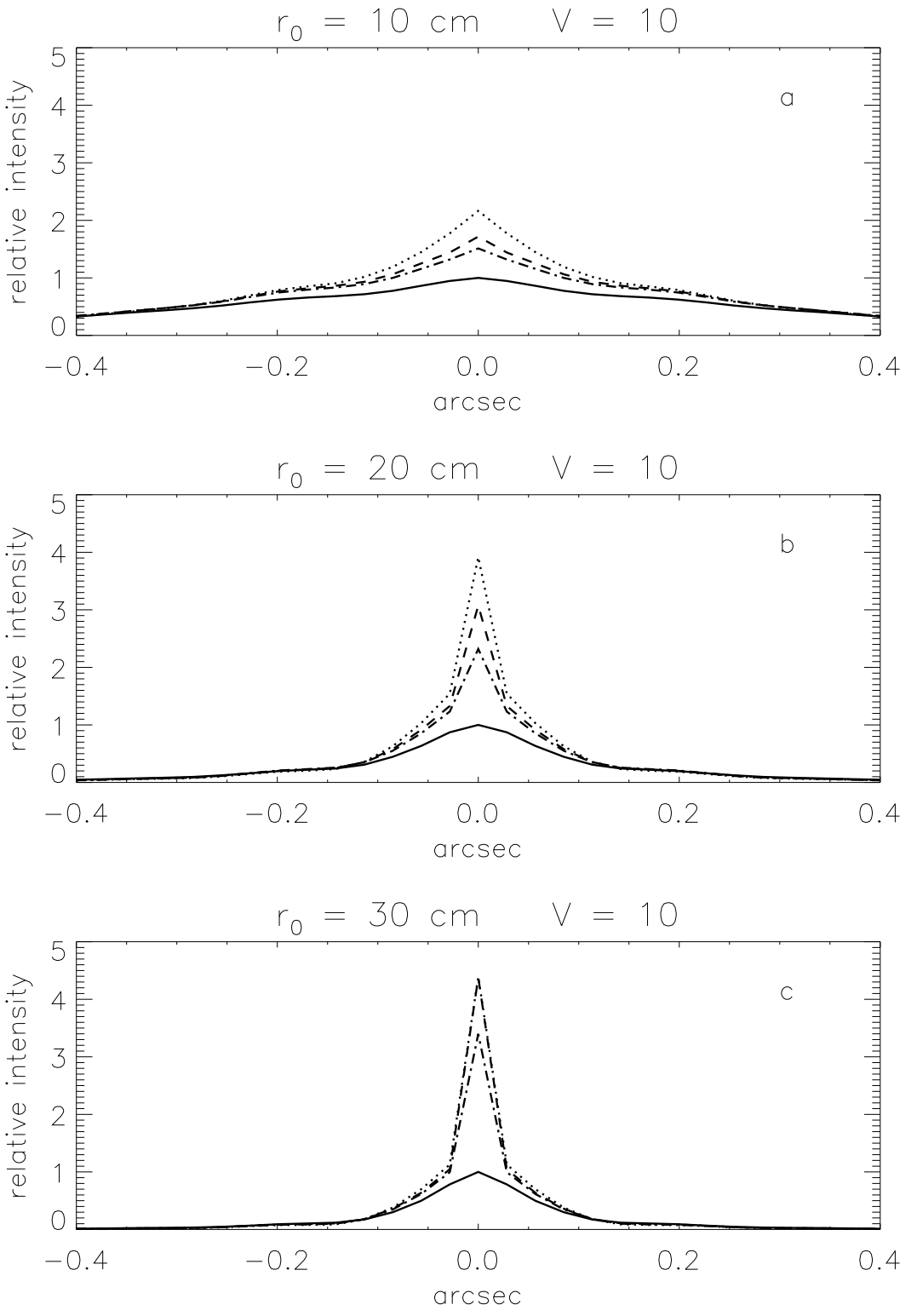

Figure 3: Radial profiles of 100% (solid line), 50% (dot-dashed line), 30% (dashed line), and 10%(dotted line) images

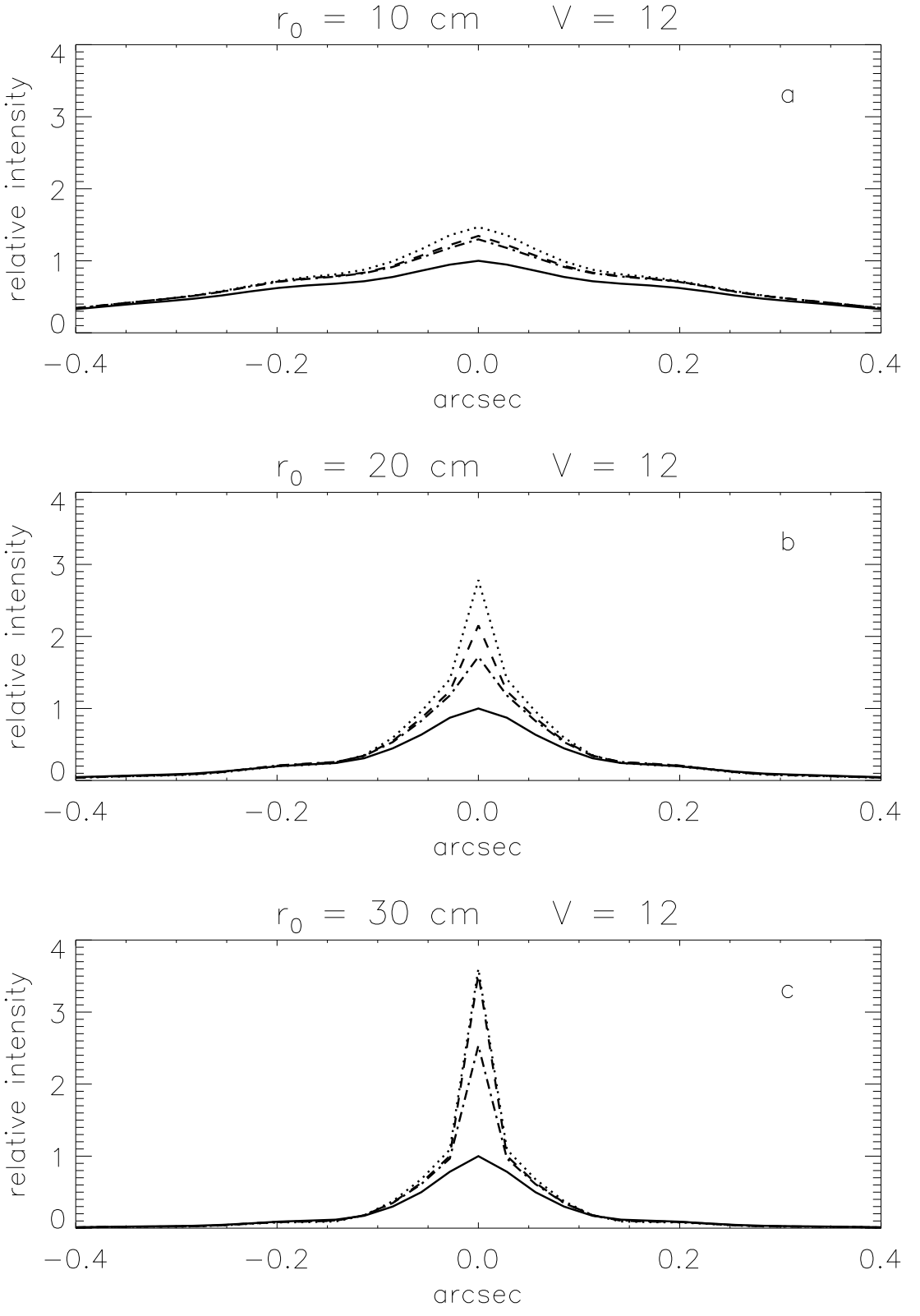

Figure 4: Radial profiles of 100% (solid line), 50% (dot-dashed line), 30% (dashed line), and 10%(dotted line) images

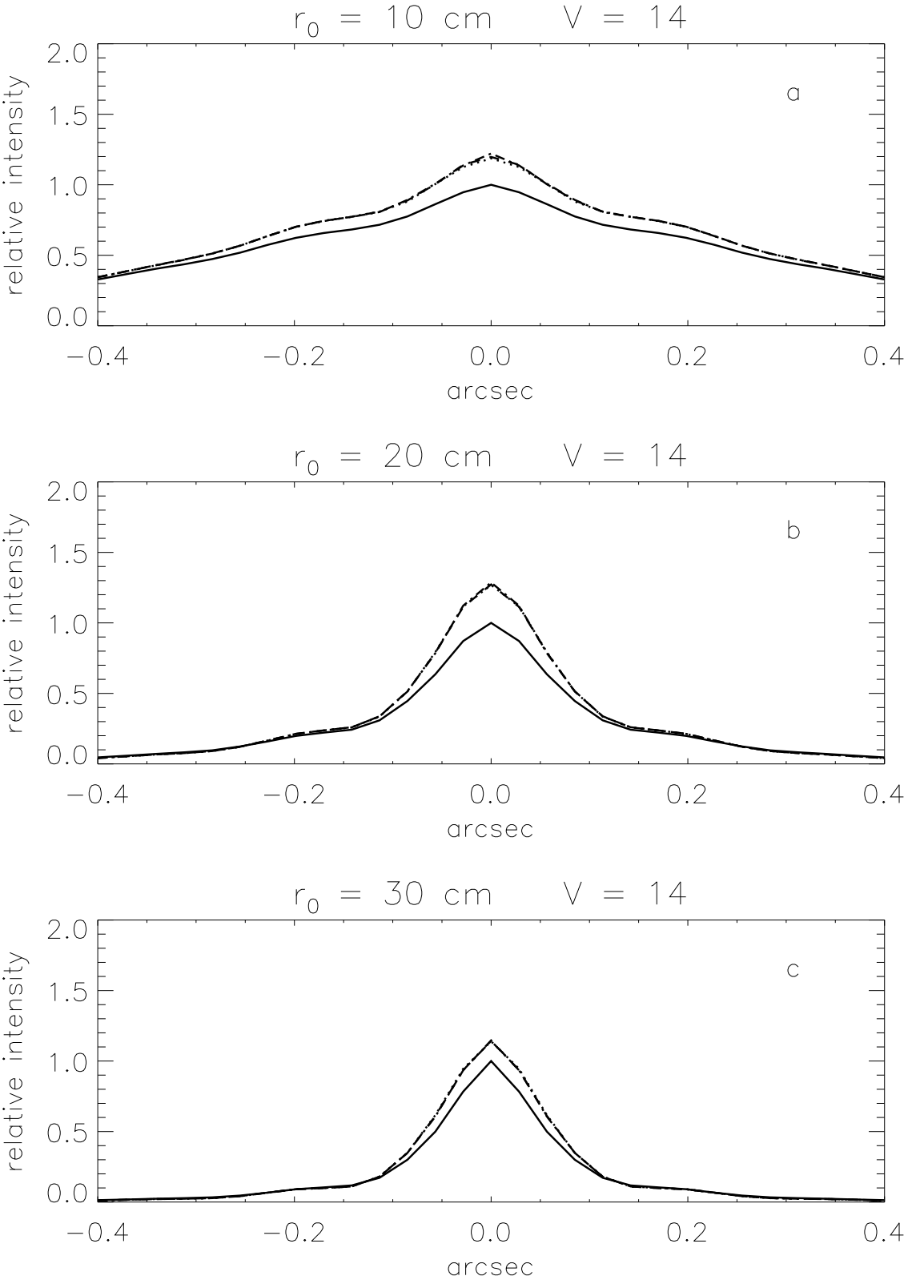

Figure 5: Radial profiles of 100% (solid line), 50% (dot-dashed line), 30% (dashed line), and 10%(dotted line) images

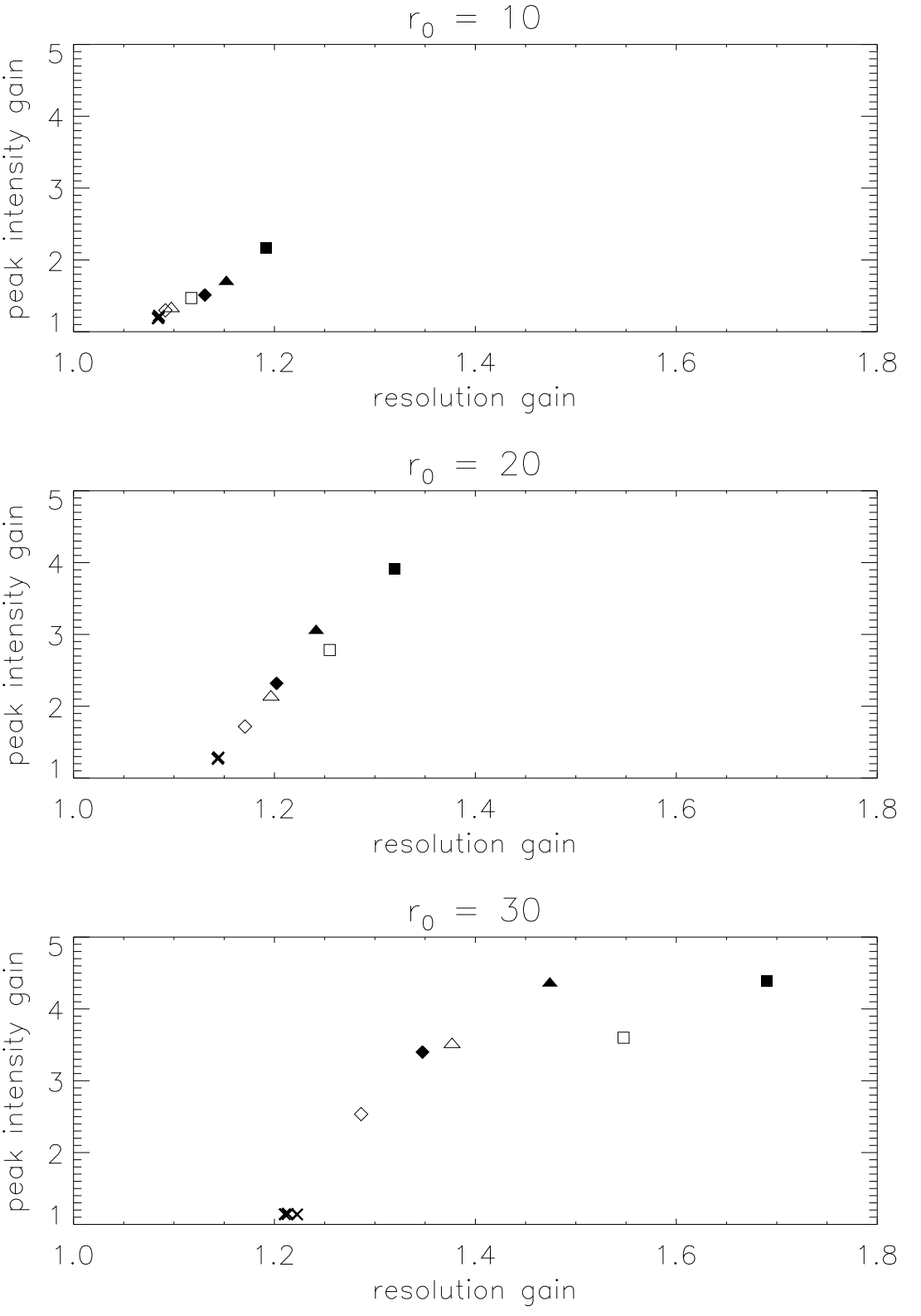

Figure 6: Peak intensity gain versus resolution gain: V=10 (10% filled box, 30% filled triangle, and 50% filled diamond), V=12 (10% open box, 30% open triangle, and 50% open diamond), and V=14 (crosses)

measure the ONMF and typical wavefront efficiency. Figures 3-6 show the comparison of the images obtained by rejecting "bad" sub-apertures with those obtained by keeping open all the sub-apertures. All the images were normalised to the same total number of photons, thus we assumed to have increased the exposure time of the 50%, 30%, 10% images by the proper factors to compensate for the minor throughput due to the "bad" sub-apertures rejection. Figures 3-5 show the radial profiles for the different V magnitudes assuming as unity the peak intensity of the 100% image. Panels a, b and c correspond to different seeing conditions. It can be seen that the on-line sub-aperture selection provides sharper images for r0=0.2, 0.3-m and V=10, 12 (panels 3b, 3c, 4b, and 4c); the improvement in the image quality is much lower for r_0=0.1-m and V=10 (panel 3a) and practically disappears for V=14 irrespectively of r_0 (panels 5a, 5b, and 5c). Figure 6 shows the peak intensity improvement (PI_g) versus the resolution gain (R_g). The peak intensity improvement and the resolution gain are defined as:

$$PI_g = \frac{PI_{sel}}{PI_{100\%}} \qquad R_g = \frac{EE_{100\%}}{EE_{sel}}$$

where $PI_{100\%}$ and $EE_{100\%}$ are the peak intensity and the 50% encircled energy diameter of the 100% image and PI_{sel} and EE_{sel} are the peak intensity and the 50% encircled energy diameter of the 50%, 30%, 10% images.

Figure 6 shows that:

i. No significant improvement either in PI_g or in R_g can be obtained with V=14. This fact is due to the dominance of Poisson noise that affects the ONMF measurements;
ii. The higher r_0, the higher are PI_g and R_g;
iii. The stricter the selection, the higher are PI_g and R_g.

In conclusion, our results show that significant improvement both in Strehl ratio and spatial resolution can be obtained in the visible for a large diameter telescope by adding on-line image selection capability to an infrared AO system. In fact, the intrinsic limitation due to the large D/r0 ratio can be overcome by adopting a multi-sub-aperture approach.

5 Acknowledgements

Partial support from the Italian MURST is acknowledged.

6 References

Fried D., 1966, JOSA, **56**, 1372.
Hecquet, J., Coupinot, G., 1985, J. Optics, Vol. 16, 21.
Muller, R.A., Buffington, A., 1974, JOSA **64**, 1200
Welsh, B.M., 1997, SPIE, Vol. 3125, 327.